JOURNAL OF AIRCRAFT
Vol. 36, No. 4, July–August 1999

Effects of Leading- and Trailing-Edge Gurney Flaps on a Delta Wing

Lance W. Traub* and Samuel F. Galls†
Texas A&M University, College Station, Texas 77843-3143

An experimental wind-tunnel investigation is undertaken to determine the effects of Gurney flaps on a 70-deg planar delta wing. Both upper- and lower-surface leading-edge, as well as trailing-edge flaps are investigated. Results are presented comprising force balance, on- and off-surface flow visualization as well as flowfield surveys. The data indicate that the lower surface leading-edge flaps increase the maximum lift coefficient and poststall lifting ability. The trailing-edge Gurney flap shifts the zero-lift angle of attack negative, thereby increasing lift for a given angle of attack, and also increases the maximum and poststall lift coefficient. Both of these flap configurations improve the wing efficiency at moderate to high lift coefficients. The devices do not greatly affect the longitudinal stability of the wing, although the trailing-edge flap generates an increase in nose-down pitching moment. The lower-surface leading-edge flap causes a moderate delay in the onset and progression of vortex breakdown over the wing. Upper surface leading-edge flaps degrade performance.

Nomenclature

C_D	= drag coefficient, D/qS_w
C_L	= lift coefficient, L/qS_w
C_m	= pitching-moment coefficient, $M/qS_w\acute{c}$
c	= wing root chord
$\acute{c}$	= mean aerodynamic chord
D	= drag
H	= stagnation pressure loss, $(P_{st} - P_\infty)/q$
h	= height of flap
k	= induced efficiency factor, $(C_D - C_{D\min})\pi AR/C_L^2$
L	= lift
M	= pitching moment
P	= pressure
q	= freestream dynamic pressure
S	= local semispan
Ste	= wing semispan
S_w	= wing planform area
x	= chordwise coordinate
z	= vertical coordinate
y	= spanwise coordinate
α	= angle of attack
$\alpha_{BD\text{-}TE}$	= angle of attack at which vortex breakdown occurs at the wing trailing edge

Subscripts

max	= maximum
min	= minimum
st	= stagnation
ZL	= zero-lift angle of attack

Introduction

THE ability of the delta-wing planform to satisfy the disparate requirements of low wave drag at high speed, coupled with stable and controllable flight at high α, have led to its widespread use and study as an effective configuration. However, these wing forms are not without limitations. Delta wings are poor lift generators, requiring high α (with consequent high drag) for takeoff and landing. If the delta wing is sharp edged, lift is augmented by suction induced by conical vortices formed above the wing from the roll-up of the shear layer emanating from the wing's leading edge. This so-called vortex lift is necessarily at the expense of a loss of leading-edge thrust; this thrust is effectively rotated through 90 deg, thus contributing the vortex lift, as shown by Polhamus.[1] On delta wings with a profiled or blunt leading edge, vortex-induced lift enhancement effects are delayed until leading-edge crossflow separation results in vortex formation.[2]

At moderate to high α, depending on the delta wing's AR, undesirable phenomena in the form of an abrupt change of the vortex structure may occur. This so-called vortex breakdown (BD) or bursting is associated with an abrupt deceleration of the vortex core, with a concomitant increase in the diameter of the resulting structure. Increasing leading-edge sweep generally delays the initial onset of vortex BD at the wing's trailing edge. The shape of the wing leading edge, i.e., symmetrical, windward or leeward beveled, or blunt,[3] also affects the onset and progression of BD over the wing, as does wing camber.[4] For high-AR wings, vortex BD has a small effect on lift until BD reaches the wing apex. For more highly swept deltas (AR < 1.46), BD has a more immediate effect on lift and usually initiates a reduction in the lift coefficient with increasing α beyond $\alpha_{BD\text{-}TE}$. For most ARs, however, BD can cause longitudinal destabilization as a result of a reduction in vortex suction over the rear of the wing.

Numerous devices have been tested with the purpose of enhancing the performance of delta wings. The most successful of these is the leading-edge vortex flap.[5–7] These devices are formed by rotating a leading-edge flap either above or below the plane of the wing. They differ from conventional leading-edge flaps in that they are not intended to suppress separation; rather, they concentrate the induced suction of the leading-edge vortex on the flap. As a consequence, drag of the wing is reduced if the flap is rotated below the plane of the wing. Lift, however, also is diminished because of a reduction in the vortex strength and a moderate reduction of the attached flow lift component. As the flaps provide leading-edge camber, they shift the angle of attack for zero-lift positive, so additionally reducing lift for a given α below stall. However, this effect does result in improved high α performance, the maximum lift coefficient peak occurring at higher α (Ref. 5). Performance of a wing with vortex flaps improves overall because the reduction in drag outweighs the loss of lift.

Apex fences (small, slender upper-surface spoilers) were conceived as devices capable of modulating the lift and pitching moment of delta-type planforms independently of the wing's angle of attack. At low angles of attack, fence deployment augments lift by

Received 7 December 1997; revision received 17 February 1999; accepted for publication 18 February 1999.

*Postdoctoral Research Associate, Aerospace Engineering Department. Associate Member AIAA.

†Graduate Student, Aerospace Engineering Department. Associate Member AIAA.

the formation of a strong fence vortex, thus potentially decreasing the landing speed of delta-winged aircraft.[8] The fences also augment pitch-down ability of the delta wing at high α (Ref. 8) by attenuating lift over the apex region of the wing. Studies also have been undertaken to determine the ability of apex and leading-edge fences to suppress wing rock.[9]

It has been shown by Liebeck[10] and others[11–13] that a trailing-edge flap comprising a small plate, typically less than 2% of the chord, can significantly enhance lift. This so-called Gurney flap usually is mounted perpendicular to the trailing edge on the pressure side. Depending on the configuration, drag also may be reduced compared to that for a wing with no flap at high C_L, resulting in improvements in the lift-to-drag (L/D) ratio. The reason for the effectiveness of the Gurney is not clear; however, the flap does increase the wing's camber at the trailing edge. The Gurney flap also may decrease the extent of flow separation near the trailing edge by increasing the downward momentum of the fluid leaving the trailing edge, which consequently enables the flow over the suction side to resist the adverse pressure gradient associated with the Kutta condition.[12]

Divergent trailing-edge (DTE) aerofoils[14,15] have been designed to reduce the drag of supercritical aerofoils in the transonic flight regime. These blunt trailing-edged profiles significantly increase lift and base drag over a similar profile with a sharp trailing edge, for a given α. However, the net effect of the DTE is an increase in the L/D ratio for a given C_L. The increased circulation from the DTE modification has been attributed to an increase in the recirculation zone downstream of the blunt trailing edge.[15] This has the effect of increasing the aerofoil's chord. Similarity between the Gurney flap and the DTE is apparent, with both devices increasing the lower-surface recompression near the trailing edge, increasing upper-surface suction for a given α, and displaying aft loading carried almost to the trailing edge. Imposition of the Kutta condition is not clear for both modifications. Consequently, the mechanism of operation of the DTE described earlier also may be present in the functioning of the Gurney flap. One of the most favorable characteristics of this flap is its simplicity compared to that of conventional high-lift devices. Subsequent studies of Gurney-inspired devices[16] have verified their effectiveness. Bloy et al.[16] have demonstrated that rearward-inclined Gurney-type flaps can improve performance more efficiently than the standard Gurney configuration.

The use of a Gurney flap to augment the lifting ability of a delta wing is an obvious progression, given its ease of application and mechanical simplicity. Buchholz[17] determined the effect of a Gurney flap on a 60-deg delta wing, as well as leading-edge fences. He found that the flaps enhanced lift but generated a significant nose-down pitching moment.

The effect of Gurney-style flaps, mounted on the leading edges as well as trailing edge of a 70-deg leading-edge sweep delta is described. The leading-edge Gurney flaps extended the entire length of the wing's leading edge and were mounted both above and below the plane of the wing, as shown in Fig. 1a. A small leading-edge Gurney flap may augment performance by providing localized leading-edge camber, and by manipulating the shear layer shed from the leading edge. Furthermore, the effects of Gurney flaps on a 70-deg-sweep delta wing are needed to extend the database on these devices. Consequently, a wind-tunnel investigation comprising force balance, on- and off-surface flow visualization, as well as flowfield surveys was undertaken.

Experimental Equipment

A mild steel delta wing with a leading-edge sweep angle of 70 deg, as detailed in Fig. 1a, was used. The wing was 1.52 mm thick and had a root chord of 400 mm, yielding a wing-thickness-to-chord ratio of 0.38%. Because the wing was thin, it was not considered necessary to bevel the edges. The flaps (see Fig. 1a) were made from thin sheets of brass and were attached with tape. For each flap variation, two flaps were tested, with flap heights ranging between 0.5 and 0.95% of the wing root chord.

The tests were undertaken in Texas A&M University's 3×4 ft continuous wind tunnel. This tunnel has a turbulence intensity of 0.3% at a freestream velocity of 42 m/s. A six-component Aero-

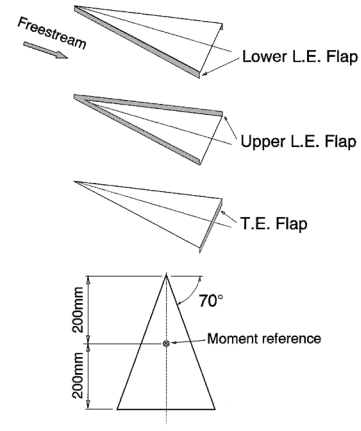

a) Model geometry showing Gurney flap variations

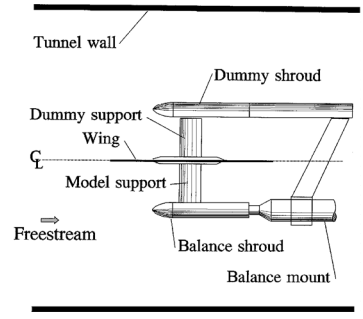

b) Model tare and interference setup

Fig. 1 Experimental details.

lab sting balance was used for force and moment determination. The accuracy of the balance is estimated at 0.6% of full scale for lift, drag, and pitching moment. Balance resolution is better than 2×10^{-4} of the measured coefficient on all channels. Repeatability of the balance for lift, drag, and pitching moment is estimated at $\Delta C_L = 0.0008$, $\Delta C_D = 0.0005$ and $\Delta C_m = 0.0008$. Model angle of attack can be set to within 0.05 deg. Freestream velocity was measured using a pitot static tube. Differential pressure was measured using an Air Neotronics digital manometer. Force balance data were acquired using a personal computer equipped with a 16-bit A/D board. Each data channel was sampled 1000 times and averaged. The data acquisition code graphically displays real-time lift, drag, and pitching moment.

The model was pitched through a set angle-of-attack range from 0 to 56 deg. After the wing was increased to a new α, data acquisition was delayed for a short time to eliminate any transient flow effects. Pitching moment was taken about 0.25 of the wing's mean aerodynamic chord. The moment reference length was the mean aerodynamic chord. Solid and wake blockage were corrected for using the method of Shindo.[18] Corrections for downwash were applied using the method detailed by Pope and Rae.[19] Figure 1b shows the sting balance mount with an installed image system consisting of a dummy shroud and support so as to facilitate determination of tare and interference. The model mount consisted of a thin streamlined support, which connected to a reinforcing spine. The model was in turn attached to the spine. The spine was used to eliminate any chordwise cambering of the model under load. The mounting system was designed to minimize balance deflections and to reduce potential interaction between the wing vortices and the balance mount. Tare and interference effects were determined using the method detailed in Ref. 19. For the present model and mount, tare and interference were generally negligible.

The wind-tunnel tests were run at a freestream velocity of 42 m/s, yielding a Reynolds number based on the wing's centerline root chord of 1.12×10^6. A Kiel probe was used for the stagnation pressure surveys. The probe had a diameter of 1.6 mm. Surveys were undertaken at $x/c = 0.7$, with the probe tracing a rectangular circuit

perpendicular to the wing surface at $\alpha = 20$ deg. The survey grid extended laterally from 0.35 to 1.1 of the semispan, and extended vertically from 0.02 z/S to 0.65 z/S. A 30×30 grid was used, yielding a point spacing of 2.6 mm in y and 2.3 mm in z. Surveys also were undertaken in the wake at $x/c = 1.4$ at the same α, with the probe oriented in a wind axis reference frame. The wake grid extended from $y/Ste = 0.35$ to 1.24, and from $z/S = -0.98$ to 0.19, with z measured from the trailing edge. The lateral and vertical grid spacing was 4.4 and 5.9 mm, respectively.

Both on- and off-surface flow visualization were undertaken. The on-surface visualization was accomplished using titanium dioxide suspended in a mixture of kerosene and linseed oil. These tests were run in the 3×4 ft tunnel at a freestream velocity of 42 m/s at $\alpha = 20$ deg. To map the vortex burst trajectories and location, water-tunnel flow visualization was undertaken. A 2×3 ft water tunnel was used, with the tests run at a freestream velocity of 0.2 m/s, yielding a root chord $Re = 80 \times 10^3$. Dye was injected at the wing apex so as to best elucidate the leading-edge vortices. Video footage was recorded during the tests and analyzed subsequently to determine the trajectories. The spiral vortex BD mode was seen to predominate, and the location of BD was taken as that at which the vortex core filament showed the distinctive kink associated with this mode.

Results and Discussion

The delta wing with no leading- or trailing-edge devices is referred to as the basic wing. Figure 2 shows a lift comparison between the basic wing and results from the studies of Wentz and Kohlman[20] and Bartlett and Vidal.[21] A theoretical prediction also is included.[22] The present results show close accord with theory and the data from Refs. 20 and 21. Figures 3a–3c present the effect of the various Gurney flaps on lift coefficient. The effect of the trailing-edgeGurney (Fig. 3a) is as would be expected for a trailing-edge device, with a significant negative shift in α_{ZL}, but a marginal change in the lift curve slope, showing that the flap primarily affects the attached flow lift component. The lift increment caused by the trailing edge flaps is seen to be proportional to the flap height. The maximum lift coefficient increases markedly, with an increase of 9.7% for the $h/c = 0.95\%$ Gurney over the basic wing. The lower leading-edge Gurney flap (Fig. 3b) is seen to have no effect on C_L until high α, where this flap form increases lift. The $h/c = 0.9\%$ lower leading-edge flap increases $(C_L)_{\max}$ by 6% over the basic wing. As shown later, this increase in the maximum lift coefficient is partly a result of a delay in the onset and progression of vortex BD over this wing configuration. The upper-surface leading-edge Gurney flap has a marginal effect on C_L as can be seen in Fig. 3c. Figures 4a–4c present the drag polars for the wings as functions of lift coefficient. Included on the plots is the lift-dependent drag

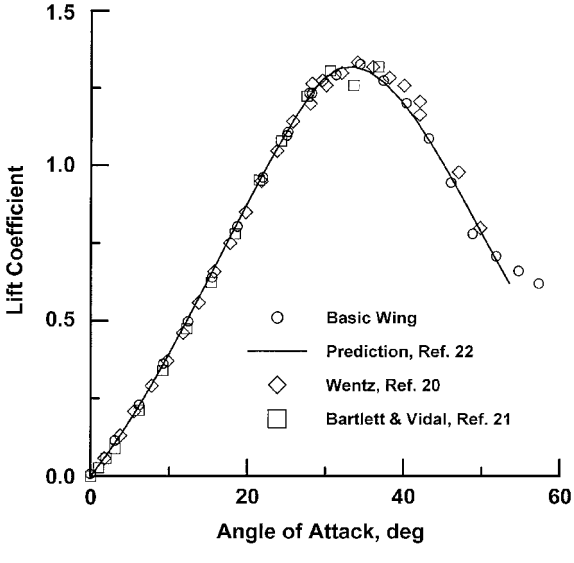

Fig. 2 Comparison of basic wing with theory and results of Refs. 20 and 21.

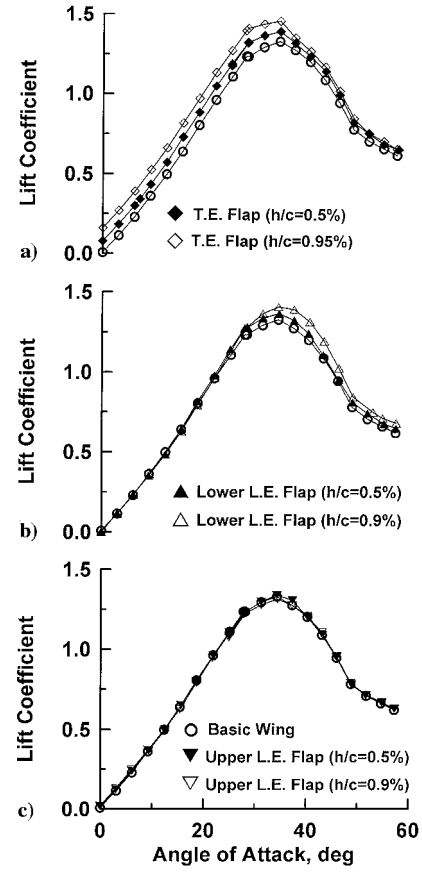

Fig. 3 Effect of Gurney flaps on lift coefficient: a) trailing-edge Gurney flap, b) lower-surface leading-edge Gurney flap, and c) upper-surface leading-edge Gurney flap.

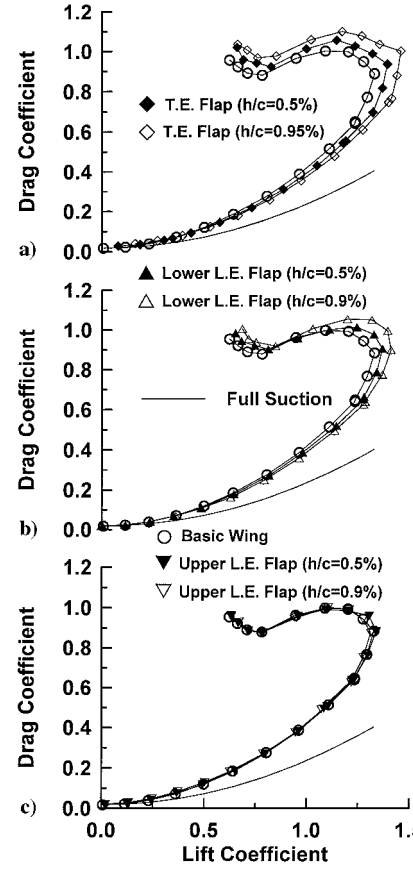

Fig. 4 Effect of Gurney flaps on drag polar: a) trailing-edge Gurney flap, b) lower-surface leading-edge Gurney flap, and c) upper-surface leading-edge Gurney flap.

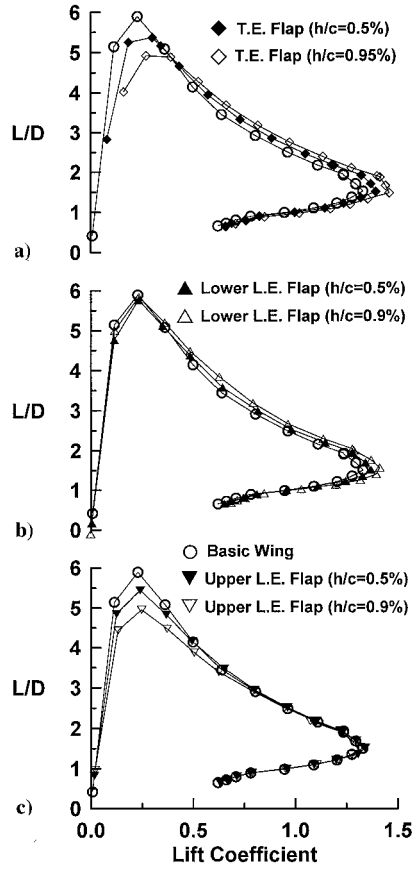

Fig. 5 Effect of Gurney flaps on *L/D* ratio: a) trailing-edge Gurney flap, b) lower-surface leading-edge Gurney flap, and c) upper-surface leading-edge Gurney flap.

value for elliptic loading and, consequently, full suction. As noted in other studies,[11] the trailing-edge Gurney flap is seen to reduce drag at moderate to high C_L (Fig. 4a), as is also seen in the plot of the lower-surface leading-edge Gurney (Fig. 4b). Inspection of Figs. 3b and 4b shows that the lower-surface leading-edge flap reduces drag at α's at which it has lifting performance equivalent to that of the basic wing. What this implies is that a certain amount of thrust must be generated on the forward facing edge of the flap to reduce drag. The upper-surface leading-edge flap is seen to have a marginal effect on C_D (see Fig. 4c).

The performance of the various flaps can be gauged effectively in terms of their L/D ratios, as presented in Figs. 5a–5c, and percentage changes in Fig. 6. Both the leading-edge lower surface and trailing-edge flaps improve L/D markedly from a lift coefficient greater than 0.28 and 0.4, respectively (see Figs. 5a, 5b, and 6). Notice that the trailing-edge Gurney does, however, incur a reduction in $(L/D)_{\max}$ compared to that of the basic wing, as a result of an increase in the minimum drag coefficient. The lower-surface leading-edge flap demonstrates practically equivalent or superior performance to that of the basic wing throughout the test range. The upper-surface leading-edge Gurney flap generally degrades wing performance for $C_L < 0.79$ compared to that of the basic wing.

Efficiency of the various flap configurations is depicted in Figs. 7a–7c, where the wing efficiency factor is shown as a function of C_L. In these plots, $k = 1$ is equivalent to the wing with full leading-edge suction and hence elliptic spanwise loading, and represents the theoretical minimum drag for a constrained-span planar wing. Note that the basic wing shows a small increase in efficiency with increasing lift coefficient. This is due to the entrainment effect of the leading-edge vortices, resulting in a substantial quantity of air being displaced downward enhancing lift for a given α. Increasing wing slenderness shows this effect of increasing wing efficiency with incidence[23] becoming more pronounced as vortex lift accounts for a greater percentage of the total lift. The trailing-edge Gurney

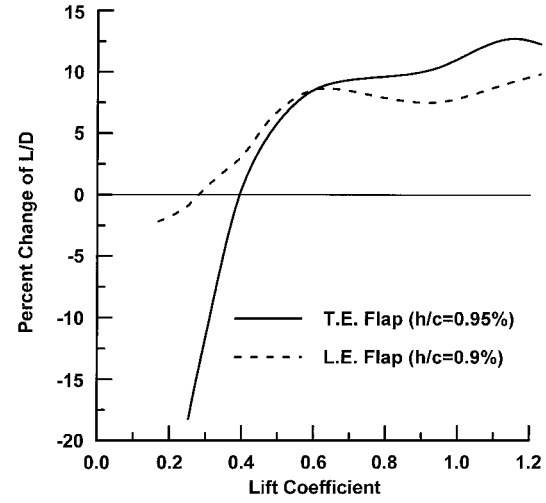

Fig. 6 Percentage increase of *L/D* of lower leading-edge and trailing-edge Gurney flap compared to that of basic wing.

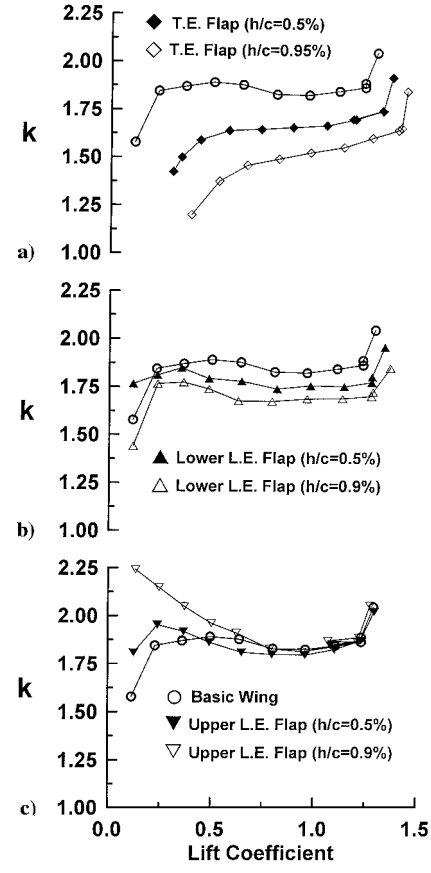

Fig. 7 Effect of Gurney flaps on wing efficiency factor: a) trailing-edge Gurney flap, b) lower-surface leading-edge Gurney flap, and c) upper-surface leading-edge Gurney flap.

flaps demonstrate a substantial improvement in efficiency compared to that of the basic wing (see Fig. 7a). This improvement is a result of the Gurney generating a substantial increase in lift for a given α, but unlike conventional trailing-edge flaps, the enhanced inviscid resultant force still acts perpendicular to the wing surface, thus avoiding a substantial increase in pressure drag that normally would occur on the aft deflected flap (assuming a sharp leading edge); i.e., lift-dependent drag is still a function of $C_L \tan\alpha$. Thus, $k = (C_L \tan\alpha)\pi AR/C_L^2$ reduces for a given C_L, if the particular C_L is generated at a lower α as is the case for the Gurney flap. The increase in efficiency of the lower-surface leading-edge flap must be as a result of thrust generation on the forward-facing extent of the flap

because this configuration has lifting performance similar to that of the basic wing for $C_L < 1.1$ (see Fig. 3b). The upper leading-edge flap generally degrades efficiency (Fig. 7c).

Thrust-generating potential of the leading-edge flaps can be elucidated by examining their ability to recover suction. The suction recovery (SR) can be defined as

$$\mathrm{SR} = \frac{\{C_L \tan\alpha - [C_D - (C_D)_{\min}]\}}{C_L \tan\alpha - \left(C_L^2/\pi AR\right)} \tag{1}$$

Equation (1) gives the measured suction as a function of the theoretical maximum attainable suction, i.e., that for a wing with elliptic loading. SR = 0 indicates zero leading-edge suction such that the resultant inviscid force on the wing is normal to the chord plane. Similarly, SR = 1 shows that the inviscid drag of the wing is the theoretical minimum for a planar constrained-span wing such that full leading-edge suction is recovered. For the basic wing and the wing with the trailing-edge Gurney flaps, SR would be zero as the resultant inviscid force on these wings is the normal force and thus $C_D - (C_D)_{\min} = C_L \tan\alpha$. Figure 8 shows SR as a function of lift for the upper and lower leading-edge flaps. As surmised earlier, the lower leading-edge Gurney flaps (Fig. 8a) do recover suction, with increasing flap size showing an increase in SR for a given C_L. Note that the suction recovered decreases with increasing α. However, this does not indicate that the magnitude of the thrust force decreases with increasing α. The upper-surface flaps (Fig. 8b), display the ability to recover some suction for $C_L > 0.25$ or 0.5 for the $h/c = 0.5$ and 0.9% flaps, respectively. For these flaps at low lift coefficients, SR probably is mitigated by localized small-scale separation on the back of the flap, thus increasing drag.

The effect of the trailing-edge Gurney flap is to increase the nose-down pitching moment for a given C_L, as shown in Fig. 9a. However, the flap does appear to increase the severity of pitch-up, i.e., the reversal of the slope of the $C_m - C_L$ curve. The increase in the moment as a result of the flap is seen to be proportional to the flap height. The effect of the upper- and lower-surface leading-edge flaps is seen to be dissimilar (Figs. 9b and 9c). The lower-surface flap reduces the nose-down moment slightly for $C_L > 0.8$, compared to that for the basic wing, whereas the upper-surface flap reduces the nose-down moment compared to that for the basic wing for $C_L < 0.8$.

Figure 10 exhibits the variation of the wing's aerodynamic center with lift coefficient for the different flaps. All configurations demonstrate a moderate forward shift of the aerodynamic center with increasing C_L. This displacement is caused by trailing-edge effects penetrating farther upstream with increasing α. The trailing-edge effects influence the vortex lift to a greater extent than the potential lift. Consequently, as the vortex lift becomes a greater constituent of the total lift with increasing α, the aerodynamic center of the wing moves forward. The trailing-edge Gurney flaps appear to shift the aerodynamic center slightly rearward compared to that of the other configurations.

Vortex burst trajectories are shown for the largest (so as to elucidate the effects of these devices clearly) of the leading-edge and trailing-edge flap configurations in Fig. 11. All configurations have

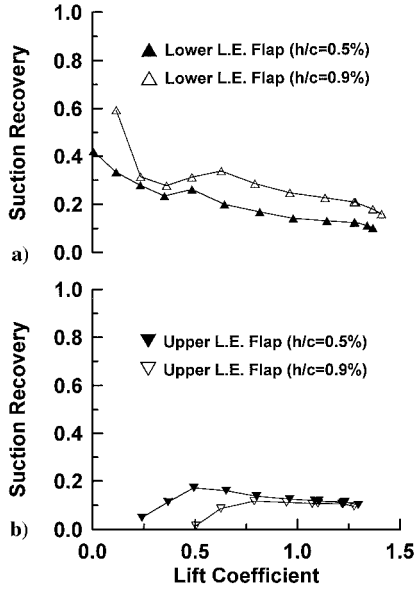

Fig. 8 Effect of Gurney flaps on leading-edge suction recovery: a) lower-surface leading-edge Gurney flap and b) upper-surface leading-edge Gurney flap.

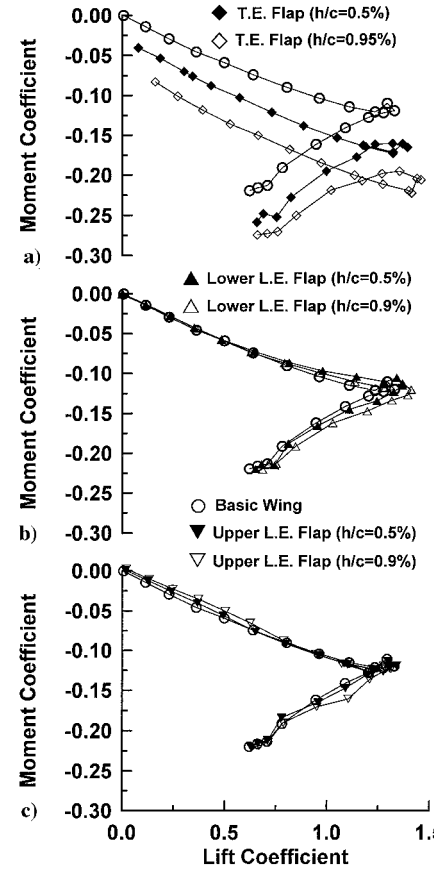

Fig. 9 Effect of Gurney flaps on pitching-moment coefficient: a) trailing-edge Gurney flap, b) lower-surface leading-edge Gurney flap, and c) upper-surface leading-edge Gurney flap.

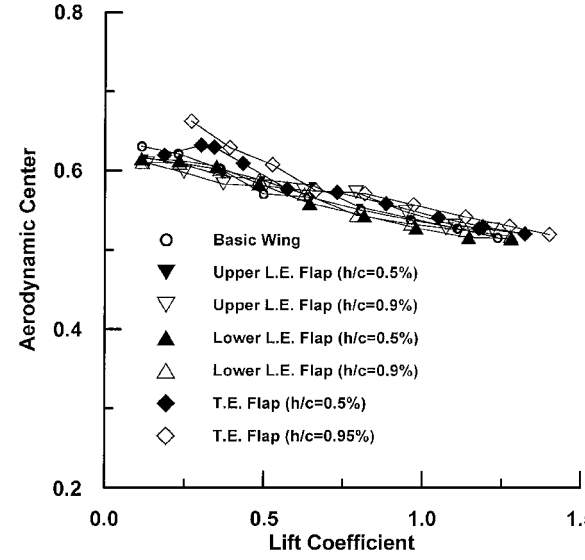

Fig. 10 Effect of Gurney flaps on location of wing aerodynamic center.

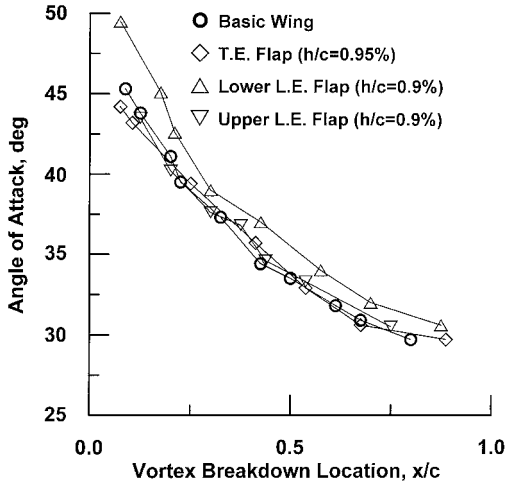

Fig. 11 Effect of Gurney flaps on vortex burst trajectory.

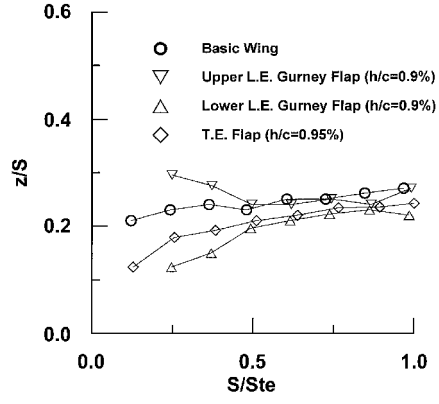

Fig. 12 Effect of Gurney flaps on vortex-core vertical trajectory.

a marginal effect on BD or its progression except the lower leading-edge flap. The lower leading-edge Gurney is seen to delay BD by approximately 2 deg. This may be due to the flap imparting a positive leading-edge camber, thus slightly weakening the vortex and so delaying BD. It is also possible that the lower leading-edge flap effectively results in the wing behaving as though it is essentially blunt edged. Kegelman and Roos[3] have shown that the effect of a blunt edge, as opposed to a symmetrically bevel-edged wing, is to delay the onset and progression of BD moderately. Their results also show an increase in $(C_L)_{\max}$ compared to a symmetrically beveled wing, similar to that noted earlier. The vertical location of the vortices above the wing for the aforementioned configurations is presented in Fig. 12 for $\alpha = 20$ deg. The data show that the lower leading-edge and the trailing-edge flaps draw the vortex closer to the wing. This would explain why weakening of the vortex by the lower leading-edge flap would not have any apparent effect on lift below $(C_L)_{\max}$, in that closer proximity of the leading-edge vortex to the wing surface would result in higher induced surface velocities and, consequently, higher suction levels. Furthermore, as shown in Fig. 3b, at $\alpha = 20$ deg, C_L of the basic wing and the lower leading-edge flap are similar, despite the closer wing–vortex proximity shown in Fig. 12. This additionally suggests that the lower leading-edge flap attenuates the vortex strength. The trailing-edge Gurney may draw the vortex closer to the surface as a consequence of increased upper surface velocities due to greater bound circulation, resulting in reduced surface pressure. The upper-surface leading-edge flap presents a physical obstacle to the vortex core near the wing apex, and thus is seen initially to displace the vortex above the position of that on the basic wing for $S/Ste < 0.54$. As the vortex moves away from the vicinity of the apex, the displacing effect decreases, and the trajectory matches that of the basic wing as shown in Fig. 12.

Flowfield surveys using the stagnation pressure probe are shown in Figs. 13a–13d for $x/c = 0.7$, $\alpha = 20$ deg. As the rate of change

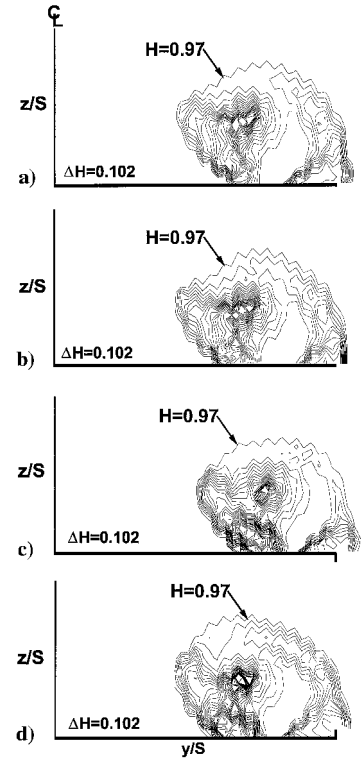

Fig. 13 Effect of Gurney flaps on vortex stagnation pressure loss ($x/c = 0.7$, $\alpha = 20$ deg): a) basic wing, b) trailing-edge Gurney flap ($h/c = 0.95\%$), c) lower-surface leading-edge Gurney flap ($h/c = 0.9\%$), and d) upper-surface leading-edge Gurney flap ($h/c = 0.9\%$).

of stagnation pressure normal to a streamline is proportional to the vorticity, the relative concentration and magnitude of vorticity can be inferred from a stagnation pressure plot. Figure 13c intimates that the vorticity and thickness of the shear layer emanating from the lower leading-edge flap are attenuated compared to those of the other configurations, which agrees with the prior suggestion that this flap may reduce the vortex strength. The reduction in the thickness of the shear layer may be partly a result of reduced interaction between the secondary vortex and the shear layer, where entrainment of fluid particles causes thickening of the primary vortex feeding sheet.[24] As shown subsequently, the lower-surface leading-edge flap causes a moderate inboard movement of the laminar secondary separation line. The chordwise location of the flow survey plane is at the approximate location of the transition from laminar to turbulent flow of the secondary separation line, such that the secondary vortex is still farther inboard than in the basic wing case, increasing its distance from the leading-edge shear layer. The shear layer also appears to be displaced outboard by the lower surface leading-edge flap, when compared to the other configurations (see Fig. 13c). The decrease in the lower-surface leading-edge flap's primary vortex shear-layer strength and thickness also may be due to the effect of the Gurney flap configuration on enforcement of the leading-edge Kutta condition. If the lower-surface leading-edge flap functions in a manner analogous to that of a trailing-edge Gurney flap, it is feasible that increased lower surface recompression[12,14] near the leading edge associated with the flap may result in reduced lower surface boundary-layer outflow velocity, causing a reduction in shear-layer vorticity.

The basic wing and trailing-edge Gurney flap show (Figs. 13a and 13b) essentially similar vortex structures and stagnation pressure distributions at this chordwise location. The upper and lower leading-edge flaps have a more pronounced effect on the structure of the vortex (see Figs. 13c and 13d). This is most marked in the stagnation pressure distribution of the upper-surface leading-edge flap's vortex core.

The stagnation pressure distribution in the wake behind the basic wing, and the trailing-edge Gurney are shown in Figs. 14a and 14b

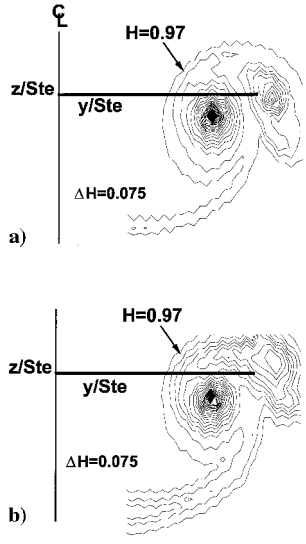

Fig. 14 Effect of Gurney flaps on vortex stagnation pressure loss ($x/c = 1.4$, $\alpha = 20$ deg): a) basic wing and b) trailing-edge Gurney flap ($h/c = 0.95\%$).

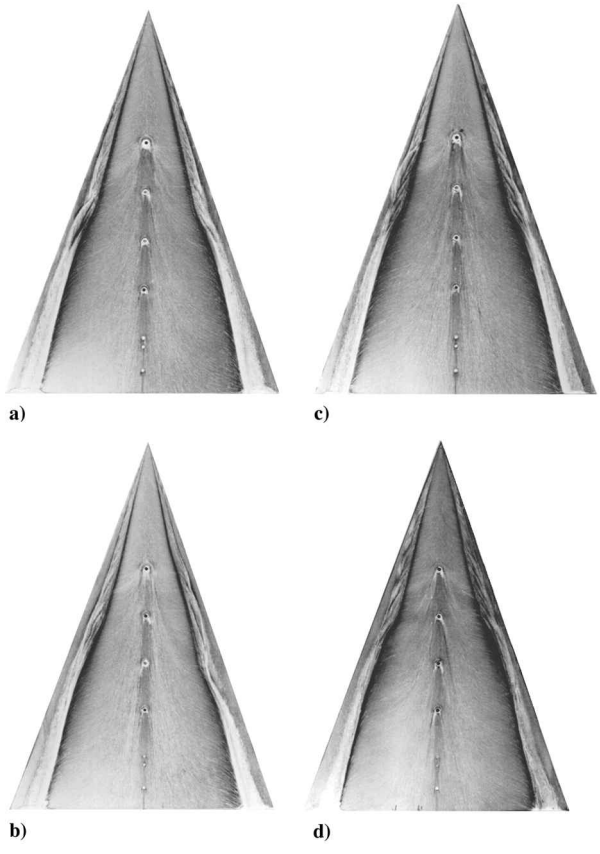

Fig. 15 Effect of Gurney flaps on limiting streamline pattern (α = 20 deg): a) basic wing, b) trailing-edge Gurney flap ($h/c = 0.95\%$), c) lower-surface leading-edge Gurney flap ($h/c = 0.9\%$), and d) upper-surface leading-edge Gurney flap ($h/c = 0.9\%$).

for $x/c = 1.4$ and $\alpha = 20$ deg. As noted for Figs. 13a and 13b, the trailing-edge flap has a marginal effect on the primary leading-edge vortex strength and structure, as also can be seen in Figs. 14a and 14b. The Gurney flap primarily affects the outer vortex, which forms due to the rolling-up of the trailing vortex sheet of the wing-bound vortex system. The flap is seen to increase the size of the partially rolled-up trailing vortex, and displaces it upward relative to the wing trailing edge. The flap significantly increases the thickness of the wake, which comprises the trailing vortex sheet imbedded in the viscous wake. The increase in the minimum drag coefficient of the trailing-edge flap is manifested in reduced wake stagnation pressure and increased wake thickness.

Figure 15 presents the limiting streamline pattern over the basic wing and the various flap configurations at $\alpha = 20$ deg. All of the patterns show probable boundary-layer transition, indicated by the kink in the secondary separation line. The configurations display a marked tertiary separation line forward of the transition location. The laminar extent of the secondary separation line for the upper and lower leading-edge Gurney flaps is situated farther inboard (approximately $0.62S$) than for the basic-wing or trailing-edge flap configurations, where the separation line is located at approximately $0.7S$. These values correlate well with those measured by Verhaagen[25] for the spanwise location of a laminar boundary layer, which, at $\alpha = 20$ deg, was determined to be approximately 65% of the local semispan. The spanwise location of the turbulent secondary separation line for the present tests (approximately $0.76S$) appears to be farther inboard than found in other studies[25,26] in which the spanwise location was approximately 0.88–$0.95S$. The lower surface flap is seen to cause asymmetric crossflow boundary-layer transition, perhaps as a result of slight variations in flap attachment (see Fig. 15c).

Conclusions

An experimental investigation is detailed that encompasses evaluation of trailing-edge Gurney flaps as well as full-span upper- and lower-surface leading-edge Gurney flaps on a 70-deg delta wing. Results are presented for force balance, flowfield survey, as well as on- and off-surface flow visualization. From the experimental data, the following conclusions are drawn: The lower-surface leading-edge flaps increase the maximum lift coefficient and poststall lift compared to those of the basic wing. The trailing-edge Gurney flap shifts the zero-lift α negative increasing lift for a given α, as well as the maximum and poststall lift. The two aforementioned configurations also improve the wing efficiency at moderate to high lift coefficients. The lower-surface leading-edge flap showed a moderate delay in the onset and progression of vortex BD over the wing. The devices do not greatly affect the longitudinal stability of the wing, although the trailing-edge Gurney caused an increase in nose-down pitching moment. Upper-surface leading-edge flaps were found to lessen performance. The results suggest that the lower-surface leading-edge Gurney flap can enhance the wing L/D ratio virtually throughout the flight regime but, unlike vortex flaps, with no concomitant lift penalty for a given α.

References

[1]Polhamus, E. C., "Prediction of Vortex Lift Characteristics by a Leading Edge Suction Analogy," *Journal of Aircraft*, Vol. 8, No. 4, 1971, pp. 193–199.

[2]Traub, L. W., "Efficient Lift Enhancement of a Blunt Edged Delta Wing," *Aeronautical Journal*, Vol. 101, No. 1002, 1997, pp. 439–445.

[3]Kegelman, J. T., and Roos, F. W., "Effects of Leading Edge Shape and Vortex Burst on the Flowfield of a 70-Degree-Sweep Delta Wing," AIAA Paper 88-4334, Aug. 1988.

[4]Lambourne, N. C., and Bryer, D. W., "The Bursting of Leading Edge Vortices—Some Observations and Discussion of the Phenomenon," Aeronautical Research Council, R&M 3282, London, April 1961.

[5]Rinoie, K., and Stollery, J. L., "Experimental Studies of Vortex Flaps and Vortex Plates: Pt. 2. 1.15m Span 60 Delta Wing," National Aerospace Lab., TR-1180T, Tokyo, Oct. 1992.

[6]Traub, L. W., "Effects of Spanwise Blowing on a Delta Wing with Vortex Flaps," *Journal of Aircraft*, Vol. 32, No. 4, 1995, pp. 884–887.

[7]Traub, L. W., "Comparative Study of Delta Wings with Blunt Leading Edges and Vortex Flaps," *Journal of Aircraft*, Vol. 33, No. 4, 1996, pp. 828–830.

[8]Rao, D. M., and Cambell, J. F., "Vortical Flow Management Techniques," *Progress in Aerospace Sciences*, Vol. 24, No. 3, 1987, pp. 173–224.

[9]Pamadi, B. N., Rao, D. M., and Niranjana, T., "Wing Rock and Roll Attractor of Delta Wings at High Angles of Attack," AIAA Paper 94-0807, Jan. 1994.

[10]Liebeck, R. H., "Design of Subsonic Airfoils for High Lift," *Journal of Aircraft*, Vol. 15, No. 9, 1978, pp. 547–561.

[11]Storms, B. L., and Jang, C. S., "Lift Enhancement of an Airfoil Using a Gurney Flap and Vortex Generators," *Journal of Aircraft*, Vol. 31, No. 3, 1994, pp. 542–547.

[12]Jang, C. S., Ross, J. C., and Cummings, R. M., "Computational Evaluation of an Airfoil with a Gurney Flap," AIAA Paper 92-2708, June 1992.

[13]Papadakis, M., Myose, R. Y., Heron, I., and Johnson, B. L., "An Experimental Investigation of Gurney Flaps on a GA(W)-2 Airfoil with 25% Slotted Flap," AIAA Paper 96-2437, June 1996.

[14]Henne, P. A., and Gregg, R. D., "New Airfoil Design Concept," *Journal of Aircraft*, Vol. 28, No. 5, 1991, pp. 300–311.

[15]Thompson, B. E., and Lotz, R. D., "Divergent-Trailing-Edge Airfoil Flow," *Journal of Aircraft*, Vol. 33, No. 5, 1996, pp. 950–955.

[16]Bloy, A. W., Tsioumanis, N., and Mellor, N. T., "Enhanced Aerofoil Performance Using Trailing-Edge Flaps," *Journal of Aircraft*, Vol. 34, No. 4, 1997, pp. 569–571.

[17]Buchholz, M. D., "Lift Augmentation on a Delta Wing via Leading Edge Fences and the Gurney Flap," NASA CR-194793, 1992.

[18]Shindo, S., "Simplified Tunnel Correction Method," *Journal of Aircraft*, Vol. 32, No. 1, 1995, pp. 210–213.

[19]Pope, A., and Rae, W. H., *Low Speed Wind Tunnel Testing*, Wiley, New York, 1984, pp. 199–208, 362–424.

[20]Wentz, W. H., Jr., and Kohlman, D. L., "Wind Tunnel Investigations of Vortex Breakdown on Slender Sharp Edged Wings," NASA CR 98737, 1968.

[21]Bartlett, G. E., and Vidal, R. J., "Experimental Investigation of Influence of Edge Shape on the Aerodynamic Characteristics of Low Aspect Ratio Wings at Low Speeds," *Journal of the Aeronautical Sciences*, Vol. 22, Aug. 1955, pp. 517–533, 588.

[22]Traub, L. W., "Prediction of Vortex Breakdown and Longitudinal Characteristics of Swept Slender Planforms," *Journal of Aircraft*, Vol. 34, No. 3, 1997, pp. 353–359.

[23]Kirby, D. A, "An Experimental Investigation of the Effect of Planform Shape on the Subsonic Longitudinal Stability Characteristics of Slender Wings," Aeronautical Research Council, R&M 3568, London, June 1967.

[24]Dagan, A., and Almosnino, D., "Vorticity Equation Solutions for Slender Wings at High Incidence," *Journal of Aircraft*, Vol. 29, No. 4, 1991, pp. 497–504.

[25]Verhaagen, N. G., "An Experimental Investigation of the Vortex Flow over Delta and Double Delta Wings at Low Speed," Dept. of Aerospace Technology, Delft Univ. of Technology, Delft, The Netherlands, Rept. LR-372, 1983.

[26]Visser, K. D., and Washburn, A. E., "Transition Behaviour on Flat Plate Delta Wings," AIAA Paper 94-1850, June 1994.